Spectral-spatial Classification of Hyperspectral Data Using Spectral-domain Local Binary Patterns

WANG Cailing[1,*], Jinchang Ren[2], WANG Hong-wei[3], Yinyong Zhang[2], WEN Jia[4]

1. Xi'an Shiyou University, School of computer science, Xi'an 710065, China
2. Department of electronic and electrical Engineering, University of Strathclyde, UK
3. Engineering University of CAPF，Xi'an,710086, China;
4. School of electronics Engineering, Tianjin Polytechnic University, Tianjin,300387,China;

Abstract- It is of great interest in spectral-spatial features classification for hyperspectral images (HSI) with high spatial resolution. This paper presents a novel Spectral-spatial classification method for improving hyperspectral image classification accuracy. Specifically, a new texture feature extraction algorithm exploits spatial texture feature from spectrum is proposed. It employs local binary patterns (LBPs) in order to extract the image texture feature with respect to spectrum information diversity (SID) to measure the differences of spectrum information. The classifier adopted in this work is support vector machine (SVM) because of its outstanding classification performances. In this paper, two real hyperspectral image datasets are used for testing the performance of the proposed method. Our experimental results from real hyperspectral images indicate that the proposed framework can enhance the classification accuracy compare to traditional alternatives.

Key Words-Hyperspectral image classification; spectral-spatial analysis; local binary patterns; spectrum information diversity; support vector machine.[1]

I Introduction

Hyperspectral image (HSI) captures reflectance values from Visible to Infrared spectrum

Received: Accepted:

Foundation: National Natural Science foundations of China (Grant Nos. 41301382, 61401439, 41604113, 41711530128) and foundation of Key lab of spectral imaging, Xi'an Institute of Optics and Precision Mechanics of CAS.

First author biography: WANG Cailing (1984-), female, lecturer, received the B.S. degree from Tianjin University in 2002, and the Ph.D. degree in Xi'an Institute of Optics and Precision Mechanics of CAS， Key lab of spectral imaging, Xi'an, China in 2011. From 2011, she is lecture in Xi'an Shiyou University. Her research interests in hyperspectral image classification and clustering. E-mail:azering@163.com

which covers a wide spectral range with hundreds of bands for each pixel in the image. This rich spectral information provides possibility to distinguish different materials spectrally. HSI classification plays an important role in hyperspectral image application, such as crop analysis, plant and mineral identification, among others.

In traditional HSI classification systems, classifiers are only able to consider spectral signatures without considering the correlations between the pixel of interest and its neighboring pixels[1, 2, 3]. Numerous classification techniques for HSI have been developed such as K-nearest-neighbor (K-NN) classifier[4] , maximum-likelihood estimation (MLE)[5], artificial neural networks[6], kernel-based techniques[7]. In particular, support vector machines [8](SVMs) have demonstrated excellent performance for HSI classification. However, it is a very challenging task due to the tiny distinction among spectral signatures of various types in same families, such as tillage in the corn fields. Meanwhile the spatial resolution is increasing during last decades, it is of great interest in exploiting spectral-spatial proposing to improve the accuracy of HSI classification[9, 10].

There are some spectral-spatial classifiers developed for Features-level fusion. For example, Generalized Composite Kernel (GCK) for combination of both spectral and spatial information were employed by multinomial logistic regression and support vector machine are introduced in[10] and[11]. In addition to the composite classifier framework, many researches focus on spatial feature extraction. For instance, morphological profiles [MPs][12] and attribute profiles [APs] [13]have been successfully employed to model structural information in hyperspectral image processing. Local binary pattern operator, which extract texture feature in spatial domain, is also used in HSI for classification [14, 15]. Meanwhile, multi-features [16] and multi-hypothesis [17]

pre-processing are present in literature.

As we all know, the texture feature is one of the key feature to display image characteristics. A batch of algorithms including gray-level co-occurrence matrix (GLCM), Gabor texture features, gradient orientation features and local binary pattern operator (LBP) are proposed to extract image texture feature such as edges, corners, and knots. Hashing methods[18][19],[20],[21], which encode high-dimensional image descriptors as compact binary strings, can be considered as new feature to be used for HSI classification. The conventional LBP is a simple yet efficient advanced operator to describe local spatial pattern by binary threshold with the center pixel value. In recent years, LBP has been widely used in image classification[22] and detection[23]. It has been proposed to be used in hyperspectral image classification recently. In [15], the LBP and Global Gabor filter(GGF) are employed to extract spatial texture information in a set of selected bands firstly, then the feature-level fusion and decision-level fusion are investigated on the extracted multiple features. Feature-level fusion combines different feature vectors together into a single feature vector. Decision-level fusion performs on probability outputs of each individual classification pipeline and combines the distinct decisions into a final one with the LOGP. Unfortunately, the LBP texture feature is extracted by calculating the histogram of local region, therefore, the time-consumption will increases rapidly with bands number increases. In order to overcome classification problem above in HSI, a new texture feature extraction algorithm which exploits spatial texture feature from spectrum domain is proposed in this paper. The proposed classification method can extract the texture feature using the algorithm proposed in this paper, then, the extracted spatial features of central pixel can be stacked with its spectral features to develop a discriminative classifier. Compared the results of experiments on two HSI datasets between the traditional LBP feature

extraction-based classification and the algorithm proposed in this paper, the proposed texture feature extraction leads to a substantial improvement in classification performance and time-consuming.

The structure of this paper is organized as follows. In section 2, we briefly introduces the previous related researches. In section 3, the proposed mathematical texture feature extraction is discussed. Section 4 provides a detailed description of the proposed classification method and also shows classification results using the real HSI. Finally, Section 5 concludes this paper with some remarks.

2. Related Work

In this section, we briefly review the conventional LBP method and SVM classifier.

A. A Review of LBP

Local binary pattern (LBP)[24] measures a local neighborhood around each central pixel whether the central pixel has a larger intensity value or not firstly, then generate a binary code for summarizing local gray-level structure. The basic LBP method considers a small circularly a small circularly symmetric neighborhood as P, along with selected neighbors $\{t_i\}_{i=0}^{P-1}$ and central pixel t_c.

The LBP is computed by:

$$LBP_{P,R(t_c)} = \sum_{i=0}^{P-1} s(t_i - t_c)2^i$$
$$s(x) = \begin{cases} 1, & x \geq 0 \\ 0, & x \leq 0 \end{cases} \tag{1}$$

Where P, R denote the number of sampling points and radius of a circle based on a circularly symmetric neighbor set of central pixel t_c. The neighboring pixels $\{t_i\}_{i=0}^{P-1}$, and $s(x)$ takes 1 if $x \geq 0$ and 0 otherwise.

After forming an LBP code image for each band of hyperspectral image, the texture feature formed as the LBP histogram is generated for each local patch centered at a pixel of interest. The time-consumption will go up rapidly with the bands number increase. To solve this problem, band selection algorithm are adopted firstly and the texture feature based on LBP is extracted from the selected bands. The PCA is most popular algorithm for dimension reduction and first one to three PC images are employed to the spatial feature extraction. Although the PCA method seems reasonable because the selected bands images are optimal for data representation, it should be noted that some important information is still contained in some other image bands.

B. SVM classifier

There are many principles to distribute the data points to a model. One of the most popular classification methods is support vector machine (SVM)[25], which is often employed for HSI image classification. The key idea behind a kernel version of SVM is to map the data from its original input space into a high-dimensional kernel-induced feature space where classes may become more separable. SVM model is constructed on determining an optimal hyper-plane in the kernel-induced space by solving

$$\min_{\omega,\xi_i,p}\left\{\frac{1}{2}\|\omega\|^2+\varsigma\sum_{i=1}^{n}\xi_i\right\} \tag{2}$$

Subject to the constraints:

$$y_i\left(\left\langle\phi\left(\omega,x_i\right)\right\rangle+p\right)\geq 1-\xi_i \tag{3}$$

For $\xi_i\geq 0$ and $i=1,...,n$, where ω is normal to the optimal decision hyper-plane (i.e. $\left\langle\omega,\phi\left(X\right)\right\rangle+p=0$), n denotes the number of samples, p is the bias term, ς is the regularization parameter which controls the generalization capacity of SVM, and ξ_i is the positive slack variable allowing us to accommodate permitted errors appropriately.

The problem above can be solved by introducing Lagrange multipliers with slack variables and regularization form

$$\max\left\{\sum_{i=1}^{n} a_i - \frac{1}{2}\sum_{i,j=1}^{n} a_i a_j y_i y_j K\left(x_i, x_j\right)\right\} \tag{4}$$

Where $a_1, a_2, ..., a_n$ are nonzero Lagrange multipliers constrained to $0 \le a_1 \le \varsigma$, and $\sum_{i=1}^{n} a_i y_i = 0$

There are some commonly implemented kernel functions like the polynomial kernel and the RBF kernel. In this paper, RBF is considered and it is represented as

$$K\left(x_i, x_j\right) = \exp\left(-\frac{\left\|x_i - x_j\right\|^2}{2\sigma^2}\right) \tag{5}$$

Finally, the decision function is represented as

$$f\left(x\right) = \operatorname{sgn}\left(\sum_{i=1}^{n} y_i a_i K\left(x_i, x\right) + p\right) \tag{6}$$

3 Texture feature for Hyperspectral image

A. Extended LBP with Respect to SID

To calculate spectrum-based LBP, we need to calculate the similarity firstly. In this paper, the Spectral information divergence (SID)[26] is employed to quantify differences between reflectance spectrums in both magnitude and direction dimensions. Some other similarity methods for two spectrums are also used in this step such as Spectral angle Cosine, etc.

Assume that hyperspectral pixel $X = (x_1, x_2, \cdots, x_L)$, each component x_l is the pixel of band B_l acquired at a particular wavelength λ_l. $\{\lambda_l\}_{l=1}^{L}$ is a set of L wavelengths. Suppose x as a random variable by defining an appropriate probability space (Ω, Σ, P) associated with it, where Ω is a sample space, Σ is an event space, and P is a probability measure.

$P=(p_1,p_2,\cdots,p_L)$ for x by

$$P(\{\lambda_l\})=p_l=\frac{x_l}{\sum_{l=1}^{L}x_l} \tag{7}$$

Denoted another hyperspectral pixel $Y=(y_1,y_2,\cdots,y_L)$ with probability $Q=(q_1,q_2,\cdots,q_L)$, vector SID is calculated by Eq. (3).

$$SID(X,Y)=D(X\|Y)+D(Y\|X) \tag{8}$$

Where $D(X\|Y)=\sum_{l=1}^{L}p_l\log(\frac{p_l}{q_l})$

Supposed that central hyperspectral pixel is X_c and the neighborhood hyperspectral pixels is $\{Y_1,Y_2,\cdots,Y_N\}$, Which N is the number of neighborhood pixels. The threshold for binary is chosen by calculating the Mean of SID, shown in Eq. (4).

$$\delta_c=\frac{1}{N}\sum_{n=1}^{N}SID(X_c,Y_n) \tag{9}$$

Then the SID_LBP is shown in Eq. (5)

$$\begin{aligned} &LBP_{N,R(X_c)}=\sum_{n=0}^{N-1}s(SID(X,Y_n)-\delta_c)2^{n-1} \\ &s(x)=\begin{cases}1, & x\geq 0\\ 0, & x\leq 0\end{cases}\end{aligned} \tag{10}$$

B. Texture Feature extraction by SID-LBP

Traditional texture feature extraction on LBP is generated for the center pixels by calculating the histograms in its corresponding local LBP image patch. The texture feature extraction on SID_LBP is also done by histograms in its corresponding local LBP image patch.

Note that patch size is a user-defined parameter, and the various patch sizes will affect the final classification accuracy.

Figure 1 illustrates the implementation of traditional LBP feature extraction and SID_LBP

feature extraction. Fig.1 (a) gives the implementation of LBP feature extraction applied to each selected band image. Fig.1 (b) gives the SID-LBP features extraction.

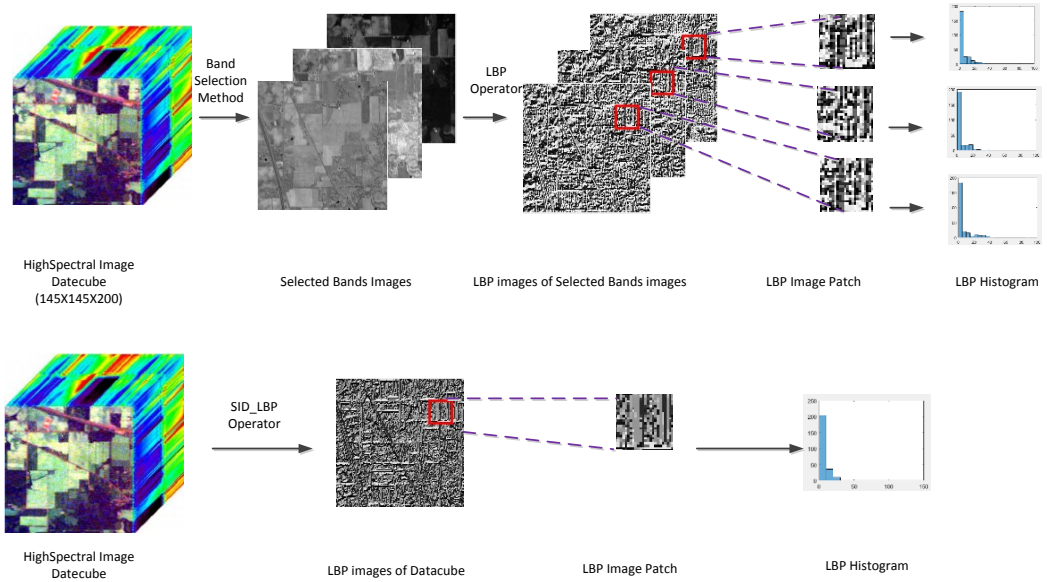

Figure 1 Comparison on implementation of traditional LBP and SID-LBP feature extraction. (a) Implementation of traditional LBP feature extraction. (b) Implementation of SID-LBP feature extraction

Compared to the conventional LBP-based classification framework, there are three main advantages on SID_LBP process. Firstly, the proposed SID_LBP texture feature extraction is done on original data cube which the total bands information are considered without any band selection methods, therefore, there is less time-consuming and less information loss. Secondly, the histogram operator obtained from each LBP image patch of every selected band image in traditional LBP feature method which the computation time will increased rapidly with the bands image number and LBP image patch size, however, the histogram calculation is only done on one image in SID_LBP operator, therefore, SID_LBP method has higher accuracy than one band selection for traditional LBP feature method and less time-consuming than multi-bands selection of traditional LBP feature. Thirdly, as all LBP histograms are stacked as texture feature for classification, the spatial feature dimensions will increase rapidly with the number of selected bands image for traditional LBP feature. SID_LBP is only done on original data cube and only one

LBP histogram is produced.

In this paper, a novel classification method is proposed, which consists of spatial texture feature by SID_LBP and classification step. The procedure is as follows.

Algorithm: SID_LBP_SVM classification

Input: Training set with N samples for each class and texture patch size sets W

Output: Classification maps and accuracy

1Calculate the texture feature histograms at window W by SID_LBP

2 Calculate spectral channel features

3 Normalize, stack and reduce spatial-spectral features

4 Train a classification model

5Classify the test set and assess accuracy

6 Return the classification maps and accuracy

4. Experimental Results

A. Data Sets

In this section, we evaluate the proposed approach using two real HSI data sets. These data sets include different contexts, different spatial resolutions and different bands in order to assess the performance of proposed approach.

The first data was collected by Airborne Visible/Infrared Image Spectrometer (AVIRIS) over Northwest Indiana, Indiana, USA, in June 1992. The image presents a classification scenario with the spatial coverage of 145×145 pixels covering 16 classes of different crops at 20-m spatial resolution and 220 bands in 0.4 to 2.45 μm region of visible and infrared spectrum. After calibrating and noisy bands were removed, 200 bands were remained to experiment.

The second data set was collected by the Reflective Optics System Imaging Spectrometer sensor covering the city of Pavia, Italy. The data set consists of 115 spectral bands with 610×340 pixels covering 9 classes with a spectral range from 0.43 to 0.86 μm and spatial resolution of 1.3 m . After removing 12 noisy channels, the remaining 103 bands were used for the test.

All the datasets present the challenging classification scenarios. The class information of three images is detailed in Table 1, Table2, and Fig.1 and Fig.2.

Table 1

The class information of Indian Pines Data set

Order	Class name	Number of samples
1	Alfalfa	54
2	Corn-notill	1034
3	Corn-mintill	834
4	Corn	234
5	Grass-pasture	497
6	Grass-trees	747
7	Grass-pasture-mowed	26
8	Hay-windrowed	489
9	Oats	20
10	Soybean-notill	968
11	Soybean-mintill	2468
12	Soybean-clean	614
13	Wheat	212
14	Woods	1294
15	Building-grass-trees-drives	380
16	Stone-steel-towers	95
	Total	10366

Table 2

The class information of Pavia Data set

Order	Class name	Number of samples
1	Asphalt	6631
2	Meadows	18649
3	Gravel	2099
4	Trees	3064
5	Metalsheets	1345
6	Bare soil	5029
7	Bitumen	1330
8	Bricks	3682
9	shadow	947
	Total	42776

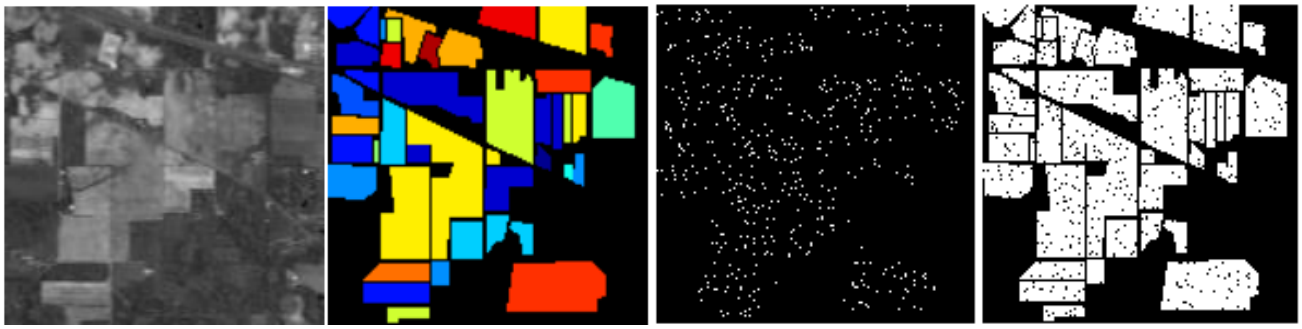

(a) (b) (c) (d)

Figure 2.The 10th band of Indian Pine image; (b) Indian Pine ground survey; (c)10% training pixels;(d) 90% test pixels

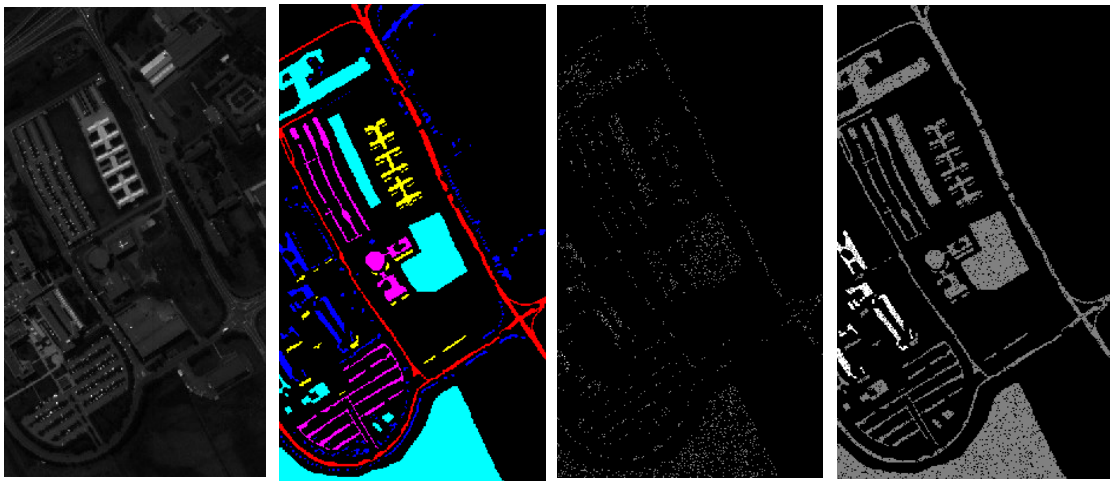

(a) (b) (c) (d)

Figure 3.(a)The 10th band of the University of Pavia;(b) the University of Pavia ground survey(c)10% training pixels;(d) 90% test pixels

B. Experimental Setup

In order to show the effectiveness of the proposed approach, the traditional LBP method is employed. There are some parameters should be considered in both traditional LBP method and SID_LBP method which is proposed in this paper. For example, the number of selected bands of images, the patch size of LBP operator and Kernel of SVM. In this paper, overall accuracy (OA), Kappa statistic (Kappa) and time consuming are estimated from confusion matrix for classification assessment. Concerning the SVM classifier, Tenfold cross-validation is employed to optimize the related parameters. The comparison is conducted on Windows 7 PC (Intel(R) Core(TM) i5-1.7GHZ 2.40GHZ with4.0GB RAM).

In order to show the performance of our proposed approach under different training

conditions and scenarios, there are two methods for training samples selection; one is selecting training samples as ratio of training samples and total samples. The ratio is range from 1% to 30 with step 1%. The other method is same number training samples in different classes with number starts from 5 to 75.

The PCA is employed for HSI dimension reduction and bands selection for traditional LBP. The impact of patch size from traditional LBP and SID_LBP is also needed to investigate. Take Indian Pine dataset as an example, when we selected the first PCs as the source, the impact of patch size on classification is shown in Fig.4.

As shown in Fig.4, it can be seen that the accuracy tends to be the maximum with 17×17 or larger. Therefore, we investigate the impact of the PCs' number with the 17×17 patch size.

To investigate the effects of number of PCs for traditional LBP, the classification accuracy and time-consuming on patch size is 17×17 with different PCs number are shown in Fig.5, Table3.

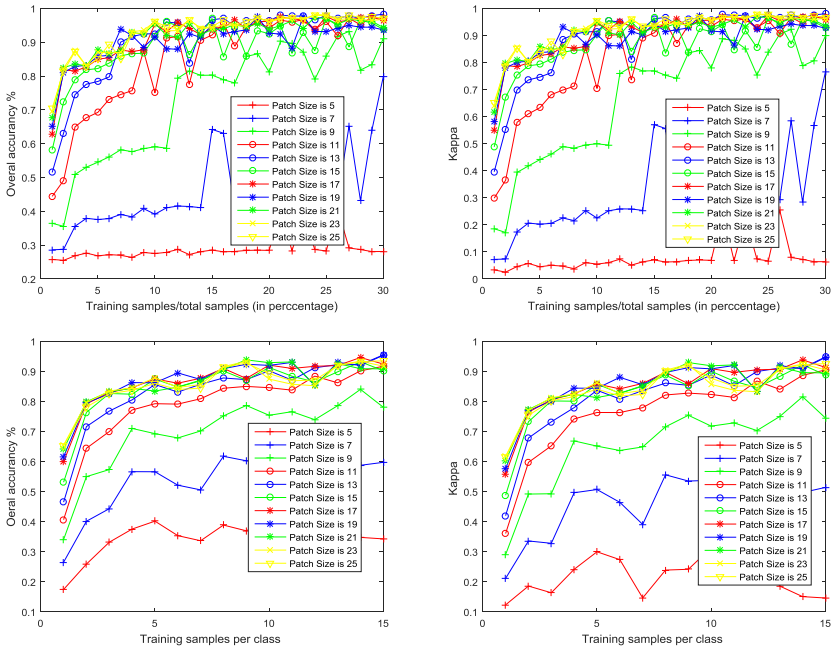

Figure 4. Classification performance versus different patch sizes and different training samples
(a)Overal accuracy versus different patch sizes and different training samples selected as ratio of training samples and total samples;(b) Kappa accuracy versus different patch sizes and different training samples selected as ratio of training samples and total samples; (c) Overal accuracy versus different patch sizes and different training samples selected same number training samples in different classes;(d) Kappa accuracy versus

different patch sizes and different training samples selected same number training samples in different classes;

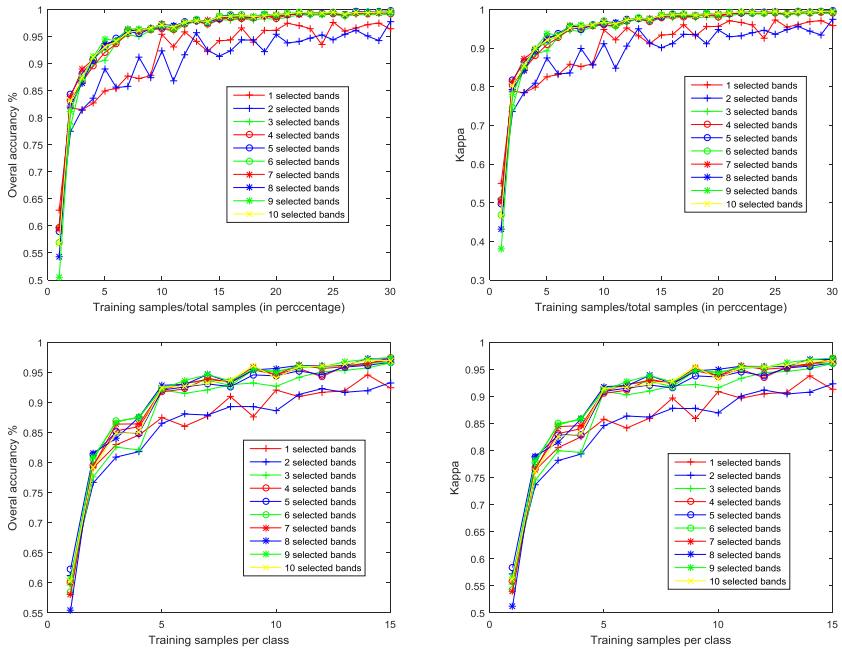

Figure 5. Classification performance versus different selected bands number and different training samples with the 17×17 patch size (a): Overal accuracy versus d different selected bands number and different training samples selected as ratio of training samples and total samples with the 17×17 patch size;(b) Kappa accuracy versus different selected bands number and different training samples selected as ratio of training samples and total samples with the 17×17 patch size; (c) Overal accuracy versus different selected bands number and different training samples selected same number training samples in different classes with the 17×17 patch size;(d) Kappa accuracy versus different selected bands number and different training samples selected same number training samples in different classes with the 17×17 patch size;

Table 3 Time-consuming versus different selected bands number and different training samples

Time-consuming (s) / Bands number / Samples selection	1	2	3	4	5	6	7	8	9	10
samples selected as ratio of training samples and total samples	0.6167	0.9934	1.4711	1.8363	2.2492	2.7788	3.1375	3.5714	4.0166	4.4571
samples selected same number training samples in different classes	0.9048	0.9983	1.3909	1.8908	2.2741	2.8497	3.0978	3.5740	4.0126	4.5305

From the Figures and Tables, we can see that the accuracy difference is not obvious above the 3 PCs. Note that the LBP features dimension and time-cost are dramatically increased with selected bands number. Therefore, we employed the 3 PCs and 17×17 patch size for traditional LBP.

C. Numerical Results

1) Classification of Indian Pines Image

In this set of experiments, we first evaluated the classification accuracy of the proposed approach using the AVIRIS Indian Pines data set in Fig.2. Table 4 shows the OAs (in percent) in traditional LBP and SID_LBP. In order to show the performance of our proposed approach under

different training conditions and scenarios, in the second experiments, we choose same training samples per class for classification assessment. Although the training samples are chosen randomly, we chosen the same training samples for comparison between two methods.

There are several conclusions can obtained from the Tables below. First of all, SID_LBP method has much better performance than original spectral signatures only. For example, in Table v, LBP-SVM (1PCs) offers 3.83% higher accuracy than the original spectrum classification in 1% training samples and 16.18% in 5 samples chosen per class. With the training samples number increase, LBP-SVM only use 1PCs offers over 20% higher accuracy than original spectrum classification; LBP-SVM (3PCs) , SID_LBP-SVM, LBP-Spe-SVM (1PCs) , LBP-Spe-SVM (3PCs) and SID-LBP-Spe-SVM offers 6.8%, 10.96%,20.23%, 21.77% and 23.96% higher accuracy individually in 1% training samples.

Secondly, spectral-spatial feature classification exhibits the potential to improve the classification results compared with using spectrum information and spatial information. For example, LBP-Spe-SVM (1PCs), LBP-Spe-SVM (3PCs) and SID_LBP-Spe-SVM which joined the spectrum and spatial information offers higher accuracy than Spe-SVM which is only using spectrum information and LBP-SVM (1PCs), LBP -SVM (3PCs) and SID_LBP-SVM which are only using spatial information.

Thirdly, the SID_LBP proposed exhibits the potential to improve the classification results than using the traditional LBP. For example, SID_LBP–SVM offers over 7.07% higher accuracy than LBP-SVM (1PCs) and 4.17% higher than LBP-SVM (3PCs) , and SID-LBP-Spe-SVM is 3.67% higher than LBP-Spe-SVM (1PCs) and 2.19% higher than LBP-Spe-SVM (3PCs) in 1% training samples; SID_LBP–SVM offers over 0.44% higher accuracy than LBP-SVM (1PCs) and

0.24% higher than LBP-SVM (3PCs) , and SID-LBP-Spe-SVM is 2.98% higher than LBP-Spe-SVM (1PCs) and 0.79% higher than LBP-Spe-SVM (3PCs) in 5 training samples per class.

Furthermore, it is noticeable that SID_LBP is more effective than traditional LBP (1PCs) and also can save more time than traditional LBP (3PCs). According to what we analyzed before, the LBP (3PCs) will extract the texture feature three times than SID_LBP method while the texture feature is done by calculating the histograms which is time-consuming.

Finally, it is observed that the obtained results which involved the spatial information are much better than the spectral information alone. This demonstrates that LBP is a highly discriminative spatial operator.

We also can get information that the SID_LBP method gets less and less effeteness with the samples number increases.

Table 4 Overal classifications accuracy (in percent) obtained for different classification methods when applied to the AVIRIS Indian Pines Hyperspectral data set using different percent training samples

Samples /total Samples	Spe-SVM	LBP-SVM (1PCs)	LBP-SVM (3PCs)	SID-LBP-SVM	LBP-Spe-SVM (1PCs)	LBP-Spe-SVM (3PCs)	SID-LBP-Spe-SVM
1	49.01	52.84	55.80	59.97	69.24	70.78	72.97
2	53.31	81.82	82.32	83.31	86.01	87.75	84.74
3	55.37	81.47	86.49	86.33	86.80	89.04	88.77
4	60.19	82.69	89.18	89.96	89.47	92.25	92.26
5	58.84	84.98	88.15	90.66	89.24	91.67	93.63
6	61.82	85.41	89.69	93.77	91.21	92.83	94.64
7	64.25	87.69	95.52	95.32	93.33	97.14	97.56
8	60.62	87.22	94.77	94.98	93.12	96.15	97.06
9	56.35	87.77	96.32	96.14	90.24	95.78	97.73
10	63.15	95.38	96.45	96.51	96.72	97.16	97.60
11	66.99	93.11	95.07	95.94	96.03	96.70	97.41
12	63.91	95.85	97.84	97.11	97.17	97.46	98.22
13	68.40	94.08	97.12	97.87	97.13	97.78	97.98
14	66.74	92.26	97.45	97.14	95.59	97.85	98.05
15	58.04	94.20	98.06	98.06	95.94	97.81	98.94
16	70.12	94.34	97.77	98.07	96.71	98.34	98.84
17	67.12	96.54	98.83	98.22	97.48	97.78	98.75
18	72.91	94.00	97.86	98.05	96.93	98.73	99.06
19	70.60	96.08	98.04	98.36	97.60	98.75	98.48
20	60.35	96.16	98.08	98.18	96.94	97.81	99.32
21	72.69	97.44	98.34	98.56	98.47	99.21	99.12
22	66.47	97.02	98.85	98.99	97.43	98.60	99.29
23	71.69	96.46	98.60	98.95	97.63	98.81	99.10
24	67.71	93.48	98.47	98.99	96.39	98.35	99.49
25	73.17	97.66	98.97	99.13	98.32	99.22	99.09
26	73.42	96.00	98.65	98.66	97.20	98.84	99.56

27	72.52	96.54	98.90	99.09	97.43	99.41	99.61
28	72.68	97.22	98.59	98.98	97.99	98.81	99.52
29	64.79	97.48	99.24	99.33	97.75	99.10	99.52
30	76.22	96.36	99.71	99.72	97.19	99.20	99.56

Table 5 Overal classifications accuracy (in percent) obtained for different classification methods when applied to the AVIRIS Indian Pines Hyperspectral data set using different percent training samples

Samples Per class	Spe-SVM	LBP-SVM (1PCs)	LBP-SVM (3PCs)	SID-LBP-SVM	LBP-Spe-SVM (1PCs)	LBP-SVM (3PCs)	SID-LBP-Spe-SVM
5	43.73	59.70	59.90	60.14	68.95	71.14	71.93
10	46.97	79.17	79.66	79.92	83.59	85.47	84.71
15	52.08	82.96	82.56	82.61	86.90	88.39	87.41
20	53.73	84.59	82.11	84.81	89.56	88.86	90.84
25	57.71	87.48	92.07	87.32	92.89	95.85	92.45
30	59.03	86.06	91.51	85.47	88.50	95.26	88.55
35	55.39	87.71	92.12	89.18	90.14	94.91	91.71
40	62.37	90.98	92.97	91.76	94.13	95.37	94.57
45	58.54	87.64	93.24	93.99	92.52	95.43	96.00
50	61.60	92.07	92.68	92.69	95.15	95.68	94.89
55	61.73	90.98	94.19	94.31	93.94	96.68	96.34
60	63.56	91.69	95.12	93.05	94.27	96.85	95.40
65	61.85	91.94	95.32	93.26	94.23	96.76	95.37
70	61.38	94.61	95.76	95.88	96.37	97.64	97.52
75	64.19	92.43	96.57	96.32	95.16	97.99	97.91

2) Classification of University of Pavia Image

In this set of experiments, we first evaluated the classification accuracy of the proposed approach using the ROSIS university of Pavia data set in Fig.3. Table 6 shows the OAs (in percent) in traditional LBP and SID_LBP. In order to show the performance of our proposed approach under different training conditions and scenarios, in the second experiments, we choose same training samples per class for classification assessment.

There are several conclusions can be obtained from the Tables below. First of all, With the LBP features, the performances are much better than with the original spectral signatures only; for example, in Table 6, LBP-SVM (1PCs) offers 3.94% high accuracy than the original spectrum classification in 1% training samples and 13.81% in 5 samples chosen per class. With the training samples number increase, LBP-SVM which only use 1PCs offers over 20% high accuracy than original spectrum classification; LBP-SVM (3PCs) , SID_LBP-SVM, LBP-Spe-SVM (1PCs) , LBP-Spe-SVM (3PCs) and SID-LBP-Spe-SVM offers 4.99%, 9.94%,16.95%, 18.70% and 23.80% high accuracy individually than the original spectrum classification in 1% training samples.

Secondly, spectral-spatial feature classification exhibits the potential to improve the classification results than only using spectrum information and spatial information. For example, LBP-Spe-SVM (1PCs), LBP-Spe-SVM (3PCs) and SID_LBP-Spe-SVM that join the spectrum and spatial information offers higher accuracy than Spe-SVM only using spectrum information and LBP-SVM (1PCs), LBP -SVM (3PCs) and SID_LBP-SVM only using spatial information.

Thirdly, the SID_LBP proposed exhibits the potential to improve the classification results than using the traditional LBP. For example, SID_LBP–SVM offers over 5% higher accuracy than LBP-SVM (1PCs) and 4.95% higher than LBP-SVM (3PCs) , and SID-LBP-Spe-SVM is 6.85% higher than LBP-Spe-SVM (1PCs) and 6.10% higher than LBP-Spe-SVM (3PCs) in 1% training samples; SID_LBP–SVM offers over 1.73% higher accuracy than LBP-SVM (1PCs) and 0.49% higher than LBP-SVM (3PCs) , and SID-LBP-Spe-SVM is 3.26% higher than LBP-Spe-SVM (1PCs) and 0.48% higher than LBP-Spe-SVM (3PCs) in 5 training samples per class.

Furthermore, it is noticeable that SID_LBP is more effective than traditional LBP (1PCs) and time-saving than traditional LBP (3PCs). Accordance to what we analyzed before, the LBP (3PCs) will extract the texture feature three times than SID_LBP method while the texture feature is done by calculating the histograms which is time-consuming.

Finally, it is observed that the obtained results involving the spatial information are much better than the spectral information alone. This demonstrates that LBP is highly discriminative spatial operator.

We also can get information that the SID_LBP method gets less and less effeteness with the samples number increases.

Table 6 Overal classifications accuracy (in percent) obtained for different classification methods when applied to the AVIRIS Indian Pines Hyperspectral data set using different percent training samples

Samples /total Samples	Spe-SVM	LBP-SVM (1PCs)	LBP-SVM (3PCs)	SID-LBP-SVM	LBP-Spe-SVM (1PCs)	LBP-Spe-SVM (3PCs)	SID-LBP-Spe-SVM

1	51.29	55.23	56.28	61.23	68.24	69.99	75.09
2	56.44	71.82	79.72	84.12	88.01	87.75	88.09
3	58.72	79.57	83.66	87.22	85.12	89.04	89.97
4	61.65	82.78	83.12	91.02	89.44	92.12	92.96
5	62.64	83.67	89.65	89.11	87.22	91.37	93.12
6	63.55	85.52	88.22	92.66	89.17	92.35	94.57
7	65.27	86.99	93.12	93.12	93.01	97.42	97.99
8	62.11	87.75	94.99	95.12	93.19	96.67	97.62
9	60.96	88.93	95.17	96.56	95.24	95.12	97.07
10	62.25	91.28	96.37	95.49	93.72	97.56	97.99
11	66.99	93.58	95.33	95.37	93.03	96.99	97.91
12	63.91	92.66	95.84	97.29	96.11	97.02	98.56
13	65.92	95.18	96.12	97.22	97.09	97.29	98.98
14	67.29	93.45	97.41	98.23	94.29	97.69	98.92
15	66.09	94.02	97.02	98.01	95.74	97.99	98.99
16	70.25	94.12	96.01	98.59	95.71	98.96	99.02
17	70.09	95.99	97.12	98.23	96.48	97.02	98.99
18	71.11	94.09	96.11	98.33	95.12	98.58	99.36
19	72.99	96.22	98.31	98.45	97.69	98.65	98.96
20	70.01	96.34	98.39	98.61	96.48	97.41	98.93
21	73.67	97.42	98.54	98.72	98.11	98.12	99.36
22	70.28	97.83	98.55	98.67	96.21	98.23	99.69
23	78.99	96.16	98.12	98.23	97.09	98.71	99.90
24	76.38	93.38	98.22	98.99	95.29	98.61	99.59
25	75.29	97.35	98.23	99.45	97.32	99.01	99.49
26	76.29	96.28	98.23	98.79	97.98	98.45	99.66
27	77.79	96.17	98.88	99.66	97.64	99.66	99.69
28	77.89	97.96	98.56	98.23	97.27	98.21	99.52
29	78.25	97.21	99.12	99.33	97.59	99.39	99.59
30	78.99	96.09	99.11	99.79	97.74	99.45	99.69

Table 7 Overal classifications accuracy (in percent) obtained for different classification methods when applied to the AVIRIS Indian Pines Hyperspectral data set using different percent training samples

Samples Per class	Spe-SVM	LBP-SVM (1PCs)	LBP-SVM (3PCs)	SID-LBP-SVM	LBP-Spe-SVM (1PCs)	LBP-SVM (3PCs)	SID-LBP-Spe-SVM
5	49.01	62.84	64.08	64.57	69.51	72.69	73.17
10	53.31	81.82	79.32	87.81	70.12	87.28	89.11
15	55.37	81.47	86.49	90.29	71.41	88.96	89.58
20	60.19	82.69	89.18	94.07	70.44	88.75	90.96
25	58.84	84.98	88.15	93.34	71.92	93.21	93.49
30	61.82	85.41	89.69	95.26	71.01	95.16	95.55
35	64.25	87.69	94.52	96.09	72.82	93.91	94.12
40	60.62	87.22	93.77	b96.87	71.21	95.12	95.21
45	56.35	87.77	94.32	96.89	71.91	95.99	96.65
50	63.15	95.38	96.45	97.22	72.47	95.46	95.47
55	66.99	93.11	95.07	98.18	72.93	96.92	96.99
60	63.91	95.85	95.84	97.68	74.08	95.72	95.72
65	68.40	94.08	95.12	95.18	73.28	95.48	95.37
70	66.74	92.26	95.45	97.98	73.84	97.69	97.99
75	68.04	94.20	97.06	97.16	74.21	97.76	98.01

5. Conclusion and Future research Lines

In this paper, we have developed a new texture feature extraction algorithm exploits spatial texture feature from spectrum. The method is proposed by employing local binary patterns (LBPs) to extract the image texture with respect to spectrum information diversity (SID) to measure the differences of spectrum information. Compared with the traditional LBP with the same classifier, which we choose here is SVM, we have got some results from the experiments above. First and

foremost, The performances with SID_LBP are much better than with the original spectral signatures only, which demonstrates that the LBP is a highly discriminative spatial operator; Second, spectral-spatial joint feature is doing well than spectrum only and spatial feature only, which means spatial information is also important for spectral image classification; Third, SID_LBP is more effective than traditional LBP (1PCs) and time-saving than traditional LBP (3PCs) while the performance between them is almost the same; Finally, SID_LBP method gets less and less effeteness with the samples number increases, because that the more samples provides more spatial information than spectrum aspect.

Although the results obtained are very encouraging, further experiments with additional scenes and comparison methods should be conducted. We also need to choose some other classifiers for experiments.

Acknowledgments

This work was supported in part by National Natural Science foundations of China (Grant Nos. 41301382, 61401439, 41604113, 41711530128) and foundation of Key lab of spectral imaging, Xi'an Institute of Optics and Precision Mechanics of CAS.

References

1 Richards, John A. *Remote Sensing Digital Image Analysis*. *Remote sensing digital image analysis :*. Springer-Verlag, 1986:47-54.

2 Bandos, Tatyana V., L. Bruzzone, and G. Camps-Valls. "Classification of Hyperspectral Images With Regularized Linear Discriminant Analysis." *IEEE Transactions on Geoscience & Remote Sensing* 47.3(2009):862-873.

3 Li, Wei, et al. "Locality-Preserving Dimensionality Reduction and Classification for Hyperspectral Image Analysis." IEEE Transactions on Geoscience & Remote Sensing

50.4(2012):1185-1198.

4 Ma, Li, M. M. Crawford, and J. Tian. "Local Manifold Learning-Based, -Nearest-Neighbor for Hyperspectral Image Classification." *Geoscience & Remote Sensing IEEE Transactions on* 48.11(2010):4099-4109.

5 Zenzo, Silvano Di, et al. "Gaussian Maximum Likelihood and Contextual Classification Algorithms for Multicrop Classification." *IEEE Transactions on Geoscience & Remote Sensing* GE-25.6(1987):815-824.

6 Stathakis, D., and A. Vasilakos. "Comparison of computational intelligence based classification techniques for remotely sensed optical image classification." *Geoscience & Remote Sensing IEEE Transactions on* 44.8(2006):2305-2318.

7 Tuia, Devis, et al. "Learning Relevant Image Features With Multiple-Kernel Classification." *IEEE Transactions on Geoscience & Remote Sensing* 48.10(2010):3780-3791.

8 Bandos, Tatyana V., L. Bruzzone, and G. Camps-Valls. "Classification of Hyperspectral Images With Regularized Linear Discriminant Analysis."*IEEE Transactions on Geoscience & Remote Sensing* 47.3(2009):862-873.

9 Gu, Yanfeng, et al. "Representative Multiple Kernel Learning for Classification in Hyperspectral Imagery." *IEEE Transactions on Geoscience & Remote Sensing* 50.7(2012):2852-2865.

10 Li, Jun, et al. "Generalized Composite Kernel Framework for Hyperspectral Image Classification." *IEEE Transactions on Geoscience & Remote Sensing* 51.9(2013):4816-4829.

11 Camps-Valls, G., et al. "Composite kernels for hyperspectral image classification." *IEEE Geoscience & Remote Sensing Letters*3.1(2006):93-97.

12 Benediktsson, J. A., J. A. Palmason, and J. R. Sveinsson. "Classification of hyperspectral data from urban areas based on extended morphological profiles." *IEEE Transactions on Geoscience & Remote Sensing* 43.3(2005):480-491.

13 Mura, Mauro Dalla, et al. "Extended profiles with morphological attribute filters for the analysis of hyperspectral data." *International Journal of Remote Sensing* 31.22(2010):5975-5991.

14 Masood, Khalid, and N. Rajpoot. "Texture based classification of hyperspectral colon biopsy

samples using CLBP." *Proceedings*(1945):1011-1014.

15 Li, Wei, et al. "Local Binary Patterns and Extreme Learning Machine for Hyperspectral Imagery Classification." *IEEE Transactions on Geoscience & Remote Sensing* 53.7(2015):1-13.

16 Huang, Xin, and L. Zhang. "An SVM Ensemble Approach Combining Spectral, Structural, and Semantic Features for the Classification of High-Resolution Remotely Sensed Imagery." *IEEE Transactions on Geoscience & Remote Sensing* 51.1(2013):257-272.

17 Chen, Chen, et al. "Spectral–Spatial Preprocessing Using Multihypothesis Prediction for Noise-Robust Hyperspectral Image Classification." *IEEE Journal of Selected Topics in Applied Earth Observations & Remote Sensing* 7.4(2014):1047-1059.

18 Gong, Yunchao, and S. Lazebnik. "Iterative quantization: A procrustean approach to learning binary codes." *IEEE Conference on Computer Vision and Pattern Recognition*. IEEE Computer Society, 2011:817-824.

19 Guo, Yuchen, et al. "Learning to Hash with Optimized Anchor Embedding for Scalable Retrieval." *IEEE Transactions on Image Processing*. PP. 99(2017):1-1.

20 Lin Z, et al. "Cross-View Retrieval via Probability-Based Semantics-Preserving Hashing." *IEEE Transactions on Cybernetics*. PP.99(2016):1-14.

21 Guo, Yuchen, et al. "Zero-Shot Learning With Transferred Samples." *IEEE Transactions on Image Processing* 26.7(2017):3277-3290.

22 Doshi, N. P., G. Schaefer, and S. Y. Zhu. "An Evaluation of LBP Texture Descriptors for the Classification of HEp-2 Cells." *IEEE International Conference on Systems, Man, and Cybernetics* IEEE, 2015.

23Kumar, V. Vijaya, K. S. Reddy, and V. V. Krishna. "Face recognition using prominent LBP model." *International Journal of Applied Engineering Research* 10.2(2015):4373-4384.

24Ojala, Timo, M. Pietikäinen, and T. Mäenpää. "Multiresolution Gray-Scale and Rotation Invariant Texture Classification with Local Binary Patterns." *IEEE Transactions on Pattern Analysis & Machine Intelligence* 24.7(2002):971-987.

25Melgani, F., and L. Bruzzone. "Classification of hyperspectral remote sensing images with

support vector machines." *IEEE Transactions on Geoscience & Remote Sensing* 42.8(2004):1778-1790.

26 Chang, Chein I. "An information-theoretic approach to spectral variability, similarity, and discrimination for hyperspectral image analysis." *IEEE Transactions on Information Theory* 46.5(2000):1927-1932.